# Electrical impedance characterization of normal and cancerous human hepatic tissue

Shlomi Laufer[1], Antoni Ivorra[2],Victor E. Reuter[3] ,Boris Rubinsky[1,2*], Stephen B. Solomon[4]

[1] Research Center for Bioengineering in the Service of Humanity and Society,
School of Computer Science and Engineering, Hebrew University of Jerusalem, Israel
[2] Depts. of Bioengineering and Mechanical Eng., University of California at Berkeley, California, USA
[3] Department of Pathology Memorial Sloan-Kettering Cancer Center, New York, New York
[4] Department of Radiology Memorial Sloan-Kettering Cancer Center, New York, New York
* To whom the correspondence should be addressed at <rubinsky@cs.huji.ac.il>

## Abstract

The four-electrode method was used to measure the ex-vivo complex electrical impedance of tissues from14 hepatic tumors and the surrounding normal liver from 6 patients. Measurements were done in the frequency range of 1 kHz - 400 kHz. It was found that the conductivity of the tumor tissue was much higher than that of the normal liver tissue in this frequency range (from $0.14 \pm 0.06$ S m$^{-1}$ vs. $0.03 \pm 0.01$ S m$^{-1}$ at 1 kHz to $0.25 \pm 0.06$ S m$^{-1}$ vs. $0.15 \pm 0.03$ S m$^{-1}$ at 400 kHz). Cole-Cole models were estimated from the experimental data and the four parameters ($\rho_0, \rho_\infty, \alpha, f_c$) were obtained using a least squares fit algorithm. The Cole-Cole parameters for cancerous and normal liver are ($9 \pm 4\ \Omega$ m$^{-1}$, $2.2 \pm 0.7\ \Omega$ m$^{-1}$, $0.5 \pm 0.2$, $140 \pm 103$ kHz) and ($50 \pm 28\ \Omega$ m$^{-1}$, $3.2 \pm 0.6\ \Omega$ m$^{-1}$, $0.64 \pm 0.04$, $10 \pm 7$ kHz), respectively. These data can contribute to developing bioelectric applications for tissue diagnostics, and in tissue treatment planning with electrical fields such as radiofrequency tissue ablation, electrochemotherapy and gene therapy with reversible electroporation, nanoscale pulsing and irreversible electroporation.

# Introduction

This study reports new experimental data on the complex electric properties of normal and malignant human liver tissue. Measurement of the electric impedance properties of tissue is not new and the fact that diseased and healthy tissues have different properties is well known and used in medical applications. However, the field of bioengineering in general and bioelectric engineering in particular has an abundance of theoretical or technology papers, but lacks tissue property data – in particular human tissue data. Therefore, it is our belief that any additional measured tissue data is a welcome contribution to the field. Measurements from human tissue are much more difficult to obtain and are more relevant to engineering applications. Several large scale studies have been published on electric impedance properties of healthy tissue; perhaps the largest one is that published by Gabriel in 1996 (Gabriel *et al.*, 1996a; Gabriel *et al.*, 1996b, c). That study provides data on a large number of various healthy tissues but does not deal with malignant tissues. Furthermore, the lower frequency range (below 1MHz) was not covered in depth. Gabriel's recent work (Gabriel et al., 2009) deals with this lower frequency range but once again only for normal tissue . When dealing with cancerous tissue, for which many practical applications of bioelectric engineering exist, this crucial basic data are very sparse or missing. For example, hundreds of papers have been published on EIT (electrical impedance tomography) of the breast. However, to the best of our knowledge there are only two major studies which report data on the electric properties of human breast cancer tissue (Surowiec *et al.*, 1988; Jossinet and Schmitt, 1999). More comprehensive data on cancer tissue properties would have obvious benefits as regards existing applications. Acquiring such data for the prostate and the breast is currently the focus of the Dartmouth group (Halter *et al.*, 2009b, a; Halter *et al.*, 2009c). With regards to the liver there are several new treatments for cancer which require knowledge of the electric properties of liver cancer tissue such as the treatment of cancer by radiofrequency (RF) induced thermal ablation. In this minimally invasive form of treatment, RF currents (around 400-500 KHz) are injected into the tumor to elevate the temperature through a Joule heating effect to levels that ablate it (Curley *et al.*, 1997;

Goldberg, 2001). Many computer models have been developed to simulate and explore the behavior of electric fields in tumors and normal tissues (Haemmerich *et al.*, 2003b; Liu *et al.*, 2005 ; Chang and Nguyen, 2004; Berjano, 2006 ). These models show that the ratio of healthy to malignant tissue electric conductivity has an important influence on the outcome of the treatment (Liu *et al.*, 2006; Solazzo *et al.*, 2005). These studies are crucial for understanding and planning RF treatment, but it is all the more concerning to see that the data reported are usually only of healthy tissue. A recent study (Dieter and et al., 2009) is one of the only ones to date to address the issue of the lack of data on malignant tissue , and in this context our independent study has value as adding to the findings of their work. We would like to mention that the general knowledge that electric properties of cancerous tissue differ from healthy tissue properties is not enough. For example, in the prostate, the malignant tissue has lower electric conductivity than the healthy tissue (Halter *et al.*, 2009a) whereas in the liver the malignant tissue has higher conductivity.

Our group has two particular reasons for researching the electric properties of cancerous human liver tissue. The first is a new emerging minimally invasive tissue ablation technique called Non Thermal Irreversible Electroporation (NTIRE). In irreversible electroporation, micro- to millisecond high field electric pulses are delivered to undesirable tissue to produce cell necrosis by inducing nanoscale defects in the cell membrane lipid bilayer. In the non-thermal mode the pulses are designed in such a way as to avoid substantial Joule heating- induced tissue damage due to temperature elevation. Hence NTIRE is a molecular surgery procedure, in the sense that it affects only one molecular component of the tissue – the cell membrane lipid bilayer. Details on the field can be found in a new book (Rubinsky, 2010)

Second, we have also developed a classifier- based diagnostic tool based on bio-impedance data. Elsewhere we have shown how bio-impedance can be used to classify tissue types. Although using electric tissue properties for diagnostics is not new, we believe that the classifier- based methods we develop are. It is important to recognize that in developing classifiers a large database of experimental measurements is absolutely essential. Our previous studies on designing classifiers for tissue diagnostics were

performed using computer simulations (Laufer and Rubinsky, 2009b; Laufer *et al.*, 2009) or animal models data (with no cancer) (Laufer and Rubinsky, 2009a). We used these partial substitutes for actual human tissue data, because no relevant human data are available in the literature. In the current study we provide the data needed for developing classifiers. To the best of our knowledge this work is the first to publish the permittivity (and not just conductivity) of liver cancer in the reported frequency range. While conductivity is the main property needed for RF and IRE simulations, the complex phase response can be critical when classifying tissue. In our opinion substantially more studies on human tissue data are needed to further develop the use of classifier techniques in diagnostics.

# Materials and methods

## EIS measurement

The measurements were performed using the four electrode method. The electrodes were made from 26 gauge (0.463 mm) hypodermic stainless steel needles. The needles were scratched using sandpaper to maximize their effective area and thus minimize their interface impedance (Geddes, 1972) . Two types of configurations were made and can be seen in Figure 1. In the first configuration the needles were placed in a straight line with a 2.3 mm distance between needles and a 5.5 mm exposure. The two outer needles were used for injecting current while the two inner needles were used for measuring the voltage. In the second configuration the needles were placed in a square shape with a 2.3 mm distance and a 5.5 mm exposure. The two top needles were used for current injection while the two bottom needles were used for voltage measurement. Although the first configuration gives a better SNR, since the measurement electrodes are in the line of the current electrodes, the second configuration was employed for smaller tumors because of its compact size.

All impedance measurements were performed using a custom-made impedance analyzer embedded in a single Printed Circuit Board (PCB). The impedance analyzer architecture is described in (Ivorra and Rubinsky, 2007). A total of 11 logarithmically spaced frequencies, ranging from 1 kHz to 400 kHz, were measured. Each scan of all 11 frequencies took 30 ms and each measurement was performed for at least 5 seconds. The maximum applied current was 100 μAp. The calculated current density calculated from the surface area of the electrode is 1.25 mA/cm$^2$ and the RMS value is 0.88 mA/cm$^2$.

## Bioimpedance relationships and measurement error evaluation

Bioimpedance is a diagnostic method based on the study of the passive electrical properties of biological tissues. When applying an alternating voltage, V, on a tissue the impedance, Z, is given by the ratio between this voltage and the resulting current, I; namely $V = I \cdot Z$. Alternatively we can use the admittance value, Y, which is given by $Y = 1/Z$ . Typically admittance combines conductive (G) and capacitive (C) components such that $Y = G + j\omega C$,where $\omega = 2\pi f$ and j is the complex number $\sqrt{-1}$. G and C depend on the properties of the tissue and on the geometry of the measurement. They are therefore typically separated into two parts:

$$G = K \cdot \sigma \quad and \quad C = K \cdot \epsilon_0 \epsilon_r \qquad (1)$$

where $\sigma$ is the conductivity of the tissue (expressed in S/m), $\epsilon_r$ is the relative permittivity of the tissue, $\epsilon_0$ is the permittivity of vacuum ($8.85 \times 10^{-12} F/m$) and $K$ is the cell constant, i.e., the geometric scaling factor of the measurement: cell = area/length (expressed in $m^2/m = m$). Since G and C are the measured parameters and $\sigma \; and \; \epsilon_r$ are the parameters that characterize the tissue, we first need to evaluate $K$.

In a recent study by Gabriel (Gabriel et al., 2009), the authors suggest a method to measure the cell constant and evaluate the noise of the measurement. We implemented this method and performed new measurements. The conductance of five NaCl solutions ranging from 0.001 to 0.15 M was measured (this range was chosen since it covers the range of values for the different tissues we studied). Theoretically ionic solutions such as aqueous NaCl exhibit no dielectric dispersion at frequencies below 1 MHz and the ratio between the conductivity of these different solutions is known. This means that comparing the different cell constants for different frequencies and different solutions can be used to estimate the total effect of equipment noise and that of different experimental artifacts such as electrode polarization. In this study we performed such an analysis. The measurements can be seen in Figure 2 and the results are summarized in Tables1-3. The method used was the same as that suggested by Gabriel et al. and a complete description can be found there. The only difference was that we also evaluated the phase data since phase was measured as well. It can be seen that for solutions 0.005 to 0.15 M the error was below 9% (compared to 10% in Gabriel et al.). For 0.001 M a higher error of 23% was present (compared to 67% in Gabriel et al.), but this solution has very low conductivity, much lower than that of body tissue, and therefore is not relevant to this study. It can also be seen that for the second needle configuration and a concentration of 0.15M the standard deviation is relatively high (12%). This is due to the fact that the total impedance is less than 10 ohm which is around the limits of our device. Since the liver has higher resistive values, this does not influence this experiment either. The phase of NaCl solutions at these frequencies should be zero and therefore any measured phase can be regarded as an error or artifact (e.g. electrode polarization). In general the phase was around $2^{0}$ with the exception of low NaCl concentration (0.001M) in the higher frequency range (100 kHz ~ 400 kHz). As mentioned the tissue measured had higher conductivities and consequently this did not influence our measurements.

## Tissue handling

This study was approved by the Institutional Review Board at the Memorial Sloan Kettering Cancer Center. All the tissue handling was performed in the Pathology Department under the supervision of one of the hospital pathologists. Measurements were made within 1-2 hours of tissue resection. Livers from six patients (3 female and 3 male, 4 with colon metastases and 2 with primary liver cancer) with 14 different tumors were examined. Patients were 42 to 81 years old (average age 58 ), and tumor size was between 0.8 cm to 5 cm (average 2 cm). Of the six livers one had cirrhosis. Due to the large size of the livers (around 10 cm) and some of the tumors, multiple measurement points were used. A total of 26 points of healthy liver, 32 points of cancerous liver and 7 points of cirrhotic liver were measured. An example of the measurement configuration can be seen in Figure 3.

## Cole-Cole model fitting

For the parameterization of the frequency-dependent impedance, the Cole-Cole dispersion model (Kenneth and Robert, 1941; Jossinet and Schmitt, 1999; Halter *et al.*, 2008) was used, with

$$\rho(f) = \rho_\infty + \frac{\rho_0 - \rho_\infty}{1 + (jf/f_c)^\alpha} \qquad (2)$$

where $\rho(f)$ is the complex resistivity given by $\rho = 1/\sigma^*$ where $\sigma^* = \sigma + j\omega\epsilon_0\epsilon_r$, $\rho_\infty$ is the high frequency resistivity, $\rho_0$ is the low frequency resistivity, $f_c$ is the characteristic frequency, $\alpha$ is the fractional power representing the depression of the circular arc from the x-axis.

The four parameters $(\rho_0, \rho_\infty, f_{c,}\alpha)$ were estimated with MATLAB's function fsolve using the Levenberg-Marquardt method. As in (Halter *et al.*, 2008) the quality of the estimation was evaluated using the goodness criterion:

$$\epsilon = \frac{1}{N}\sum_{i=1}^{N} |\rho_m(f_i) - \rho_e(f_i)| \qquad (3)$$

where $\rho_m(f_i)$and $\rho_e(f_i)$ are the measured and estimated impedances at each frequency, respectively, and $N$ is the number of frequencies (in our case 11).

The initial parameters were set in the following manner (Halter *et al.*, 2008):

$\rho_\infty$: Real part of impedance at the maximum frequency, 400 kHz.

$\rho_0$: Real part of impedance at the minimum frequency, 1 kHz.

$f_c$: Frequency at which $Im\big(\rho_m(f_i)\big) > Im\big(\rho_m(f_{i-1})\big)$ & $Im\big(\rho_m(f_i)\big) > Im(\rho_m(f_{i+1}))$ first occurs as the frequency proceeds from low to high $i = 2,3, \dots, N-1$.

$\alpha$: Set to 1 for all cases.

# Results

When presenting bioimpedance data using the matching Cole-Cole models two approaches can be taken. In the first approach the impedance values from all the tissue data sets are initially averaged and then these average values are used to extract the Cole-Cole parameters. In the second approach a Cole-Cole model is developed for each tissue data set and the model parameters are averaged over all the data sets. Due to variations between tissues these two methods will yield different results. Furthermore, while the first method gives the standard deviation of the impedance values, in the second method the standard deviation will be of the Cole-Cole parameters. Averaging the impedance values has the advantage of averaging the data that was actually measured and avoiding the model fitting stage, which is known to introduce errors. When examining the correlation between the different impedance values for different frequencies, we found them to be much higher (~ 0.9) than those of different Cole-Cole parameters (~ 0.45). This would suggest that when adding independent and identically distributed (i.i.d) noise to simulated data (for example in computer models) it would be better to use the Cole-Cole model and add the noise to Cole-Cole parameters and not to the impedance values. Given these considerations we decided to present the Cole-Cole parameters obtained from both methods. The average and standard deviation of the electrical conductivity and the relative permittivity can be found in Table 4 and are plotted in Figure 4. As a

reference the data for normal liver from (Gabriel *et al.*, 1996b) are also presented in Figure 4. The average impedance values can be seen in Figure 5 and the average admittance in Figure 6. The Cole-Cole parameters were also calculated for each of the measurements. The average error between the model and the measured data was $0.1 \pm 0.1\ \Omega$ (approximately 1%). A sample of these models can be seen in Figure 7, and the average and standard deviation are presented in Table 5.

# Discussion

Previous studies of the liver, both animal and human, (Smith *et al.*, 1986; Joines *et al.*, 1994; Haemmerich *et al.*, 2003a; Stauffer *et al.*, 2003; O'Rourke *et al.*, 2007; Dieter and et al., 2009) showed that cancerous tissue has higher conductivity values than healthy tissue. In our study we found the same relationship. These ratios are not trivial since in prostate cancer the tumor has lower conductivity than the surrounding healthy tissue (Halter *et al.*, 2008; Halter *et al.*, 2009b) while in breast cancer the tumor has higher conductivity than the surrounding fat typically found at older ages, but lower than glandular tissue (Jossinet and Schmitt, 1999).

It has also been found that the difference in electrical conductivity values is much higher in the lower frequency range, as reported in (Dieter and et al., 2009). In (Haemmerich and Wood, 2006; Dieter and et al., 2009) it was suggested that the RF ablation frequency (currently around 400-500 kHz) should be reduced. It was shown that although the conductivity of malignant tissue is higher at all frequencies, the difference is much higher at lower frequencies and therefore performing the ablation process at lower frequencies will cause the current to preferentially heat the malignant tissue. This will cause better destruction of the tumor with less damage to surrounding tissue. Further studies should examine impedance values on the border of the tumor. If they are closer to those of healthy tissue, then reducing the frequency might accelerate the necrosis of the center of the tumor, where lower conductivities exist, while leaving the boundary alive to regenerate. Another issue is that the difference between ablated tissue and non ablated tissue is much higher at the lower frequency range (Dieter and et al., 2009). Once again this can encourage the electrical currents and the resulting heating to concentrate in the ablated area where the electrical conductivity is higher. Although using higher

frequencies seems less efficient, the heating process might be more homogenous and thus more predictable. These parameters should be used in future computer simulations, and more ex-vivo RF ablation experiments should be performed for a better understanding of the problem.

In addition, it was seen that the β dispersion central frequency of the malignant tissue was much higher than that of the normal tissue (155.7 kHz and 10.5 kHz respectively). The β dispersion depends on the cell membrane capacity. Since regions of cell necrosis are commonly found inside tumor tissue, the capacitive effect of the intact cell membrane in those areas is reduced. As mentioned the conductivity at the lower frequency range is much higher in cancerous tissue. This could be due to higher extra-cellular water content in the tumor and lower cell membrane density due to necrosis. At the high frequency range the conductivity is still higher, although less significant than in the lower range, this would suggest intracellular changes as well.

Only one liver was cirrhotic and thus further studies need to be done. The conductivity of this liver was much higher than of the healthy liver and it had a reduced phase response in comparison to healthy tissue. The considerable difference between healthy and cirrhotic liver could suggest bio-impedance as a method for non-invasive liver evaluation (using methods similar to Electrical Impedance Tomography).

Another interesting fact was that while for all the healthy tissues a Cole-Cole model was easily fit, the frequency response for some of the cancerous tissue was "flat" and thus the model appeared not to fit. This phenomenon has been reported in previous studies (Antoni and et al., 2009; Jossinet and Schmitt, 1999) and an example can be seen in Figure 7. This could influence the relatively large variability of parameter $f_c$ in the Cole-Cole model.

The wide variability of the data in this study is a disturbing matter. We found the variability to be around 25% for healthy tissue and 40% for cancerous tissue, while the consistency of our equipment was better than 9% and on average around 5%. However, similarly large variability is not unusual and has been reported in other studies as well (Halter *et al.*, 2009a; Jossinet and Schmitt, 1999). A possible explanation can be found in Haemmerich *et al.*, 2002 which shows that the conductivity in an animal model decreases by 53% at 10 Hz and by 32% at 1 MHz during the first two hours after liver removal.

Since in a clinical setup we cannot control the exact time between removal of the liver and the time when the tissue properties are measured, this can influence the variability of the data, as was pointed out by (Halter *et al.*, 2009a). The effect of the time lag on measurement observed by Haemmerich *et al.* coincides to some extent with the fact that in our data the variability was higher at the lower frequency range. This variability in the lower frequency range, especially in the permittivity, could also be due to electrode polarization which is more dominant in this frequency range. In four of the livers we measured more than four areas and we calculated the standard deviation. We found it to be 15% for healthy tissue and 25% for cancerous tissue. Since these measurements were performed approximately at the same time this suggests that these values represent the measurement accuracy and tissue inhomogeneity whereas the remainder can be ascribed to patient variability and the time lag between tissue extraction and measurement. The larger variability in tumors is probably due to their irregular form. It was also shown in (Haemmerich *et al.*, 2002) that after 24 hours the conductivity values rise again. This could explain why on average we obtained lower values than those found by (Gabriel *et al.*, 1996b). The variability in the data further emphasizes the need for many more experimental studies on physiological measurements of human tissue data for bioimpedance applications. Further studies should also examine whether the time of ischemia affects differently malignant and normal liver tissue.

# Conclusion

The electrical conductivity and permittivity of ex-vivo malignant and healthy liver tissue was measured. It was found that malignant tissue had higher conductivity values and a lower phase response in the entire measured frequency range (1 kHz-400 kHz). These data can be used for both bio-impedance needle guidance and to improve the RF ablation procedure. In this work we did not distinguish between different types of liver cancers due to the small amount of data and IRB constraints. This should be examined in larger samples and the feasibility of using bio-impedance measurements as a classifier should be evaluated. Furthermore it would be interesting to compare malignant tumors to benign tumors; these data could be used to construct bio-impedance based tissue classifiers

316 (Laufer and Rubinsky, 2009a, b). Examining the homogeneity of impedance values over
317 the entire tumor, including its borders, could help improve the RF ablation procedure.

## References:


Andreuccetti D, Fossi R and Petrucci C 1997 Institute for Applied Physics "Nello Carrara" of the Italian National Research Council. Calculation of the dielectric properties of body tissues in the frequency range 10 Hz - 100 GHz. Florence (Italy) http://niremf.ifac.cnr.it/tissprop/

Antoni I and et al. 2009 In vivo electrical conductivity measurements during and after tumor electroporation: conductivity changes reflect the treatment outcome *Physics in Medicine and Biology* **54** 5949

Berjano E J 2006 Theoretical modeling for radiofrequency ablation: state-of-the-art and challenges for the future *Biomed Eng Online* **5** 24

Chang I A and Nguyen U D 2004 Thermal modeling of lesion growth with radiofrequency ablation devices *Biomed Eng Online* **3** 27

Curley S A, Davidson B S, Fleming R Y, Izzo F, Stephens L C, Tinkey P and Cromeens D 1997 Laparoscopically guided bipolar radiofrequency ablation of areas of porcine liver *Surg Endosc* **11** 729-33

Dieter H and et al. 2009 Electrical conductivity measurement of excised human metastatic liver tumours before and after thermal ablation *Physiological Measurement* **30** 459

Gabriel C, Gabriel S and Corthout E 1996a The dielectric properties of biological tissues: I. Literature survey *Phys Med Biol* **41** 2231-49

Gabriel C, Peyman A and Grant E H 2009 Electrical conductivity of tissue at frequencies below 1 MHz *Phys Med Biol* **54** 4863-78

Gabriel S, Lau R W and Gabriel C 1996b The dielectric properties of biological tissues: II. Measurements in the frequency range 10 Hz to 20 GHz *Phys Med Biol* **41** 2251-69

Gabriel S, Lau R W and Gabriel C 1996c The dielectric properties of biological tissues: III. Parametric models for the dielectric spectrum of tissues *Phys Med Biol* **41** 2271-93

Geddes L A 1972 *Electrodes and the measurement of bioelectric events* Wiley-Interscience: New York

Goldberg S N 2001 Radiofrequency tumor ablation: principles and techniques *Eur J Ultrasound* **13** 129-47

Haemmerich D, Ozkan R, Tungjitkusolmun S, Tsai J Z, Mahvi D M, Staelin S T and Webster J G 2002 Changes in electrical resistivity of swine liver after occlusion and postmortem *Med Biol Eng Comput* **40** 29-33

Haemmerich D, Staelin S T, Tsai J Z, Tungjitkusolmun S, Mahvi D M and Webster J G 2003a In vivo electrical conductivity of hepatic tumours *Physiol Meas* **24** 251-60

Haemmerich D and Wood B J 2006 Hepatic radiofrequency ablation at low frequencies preferentially heats tumour tissue *Int J Hyperthermia* **22** 563-74

Haemmerich D, Wright A W, Mahvi D M, Lee F T, Jr. and Webster J G 2003b Hepatic bipolar radiofrequency ablation creates coagulation zones close to blood vessels: a finite element study *Med Biol Eng Comput* **41** 317-23

Halter R J, Hartov A, Paulsen K D, Schned A and Heaney J 2008 Genetic and least squares algorithms for estimating spectral EIS parameters of prostatic tissues *Physiol Meas* **29** S111-23

Halter R J, Schned A, Heaney J, Hartov A and Paulsen K D 2009a Electrical properties of prostatic tissues: I. Single frequency admittivity properties *J Urol* **182** 1600-7

Halter R J, Schned A, Heaney J, Hartov A and Paulsen K D 2009b Electrical properties of prostatic tissues: II. Spectral admittivity properties *J Urol* **182** 1608-13

Halter R J, Zhou T, Meaney P M, Hartov A, Barth R J, Jr., Rosenkranz K M, Wells W A, Kogel C A, Borsic A, Rizzo E J and Paulsen K D 2009c The correlation of in vivo and ex vivo tissue dielectric properties to validate electromagnetic breast imaging: initial clinical experience *Physiol Meas* **30** S121-36

Ivorra A and Rubinsky B 2007 In vivo electrical impedance measurements during and after electroporation of rat liver *Bioelectrochemistry* **70** 287-95

Joines W T, Zhang Y, Li C and Jirtle R L 1994 The measured electrical properties of normal and malignant human tissues from 50 to 900 MHz *Med Phys* **21** 547-50

Jossinet J and Schmitt M 1999 A review of parameters for the bioelectrical characterization of breast tissue *Ann N Y Acad Sci* **873** 30-41

Kenneth S C and Robert H C 1941 Dispersion and Absorption in Dielectrics I. Alternating Current Characteristics *The Journal of Chemical Physics* **9** 341-51

Laufer S and Rubinsky B 2009a Cellular phone enabled non-invasive tissue classifier *PLoS ONE* **4** e5178

Laufer S and Rubinsky B 2009b Tissue Characterization With an Electrical Spectroscopy SVM Classifier *Biomedical Engineering, IEEE Transactions on* **56** 525-8

Laufer S, Solomon S B and Rubinsky B 2009 A new linear algebra based mathematical technique for Electrical Impedance Spectroscopy guided biopsy *Accepted to the 11th World Congress on Medical Physics and Biomedical Engineering*

Liu Z, Ahmed M, Weinstein Y, Yi M, Mahajan R L and Goldberg S N 2006 Characterization of the RF ablation-induced 'oven effect': the importance of background tissue thermal conductivity on tissue heating *Int J Hyperthermia* **22** 327-42

Liu Z, Lobo S M, Humphries S, Horkan C, Solazzo S A, Hines-Peralta A U, Lenkinski R E and Goldberg S N 2005 Radiofrequency tumor ablation: insight into improved efficacy using computer modeling *AJR Am J Roentgenol* **184** 1347-52

O'Rourke A P, Lazebnik M, Bertram J M, Converse M C, Hagness S C, Webster J G and Mahvi D M 2007 Dielectric properties of human normal, malignant and cirrhotic liver tissue: in vivo and ex vivo measurements from 0.5 to 20 GHz using a precision open-ended coaxial probe *Phys Med Biol* **52** 4707-19

Rubinsky B 2010 Irreversible Electroporation In *Series in Biomedical Engineering* Springer pp X1V, 314

Smith S R, Foster K R and Wolf G L 1986 Dielectric properties of VX-2 carcinoma versus normal liver tissue *IEEE Trans Biomed Eng* **33** 522-4

Solazzo S A, Liu Z, Lobo S M, Ahmed M, Hines-Peralta A U, Lenkinski R E and Goldberg S N 2005 Radiofrequency ablation: importance of background tissue electrical conductivity--an agar phantom and computer modeling study *Radiology* **236** 495-502

Stauffer P R, Rossetto F, Prakash M, Neuman D G and Lee T 2003 Phantom and animal tissues for modelling the electrical properties of human liver *Int J Hyperthermia* **19** 89-101

Surowiec A J, Stuchly S S, Barr J R and Swarup A A S A 1988 Dielectric properties of breast carcinoma and the surrounding tissues *Biomedical Engineering, IEEE Transactions on* **35** 257-63

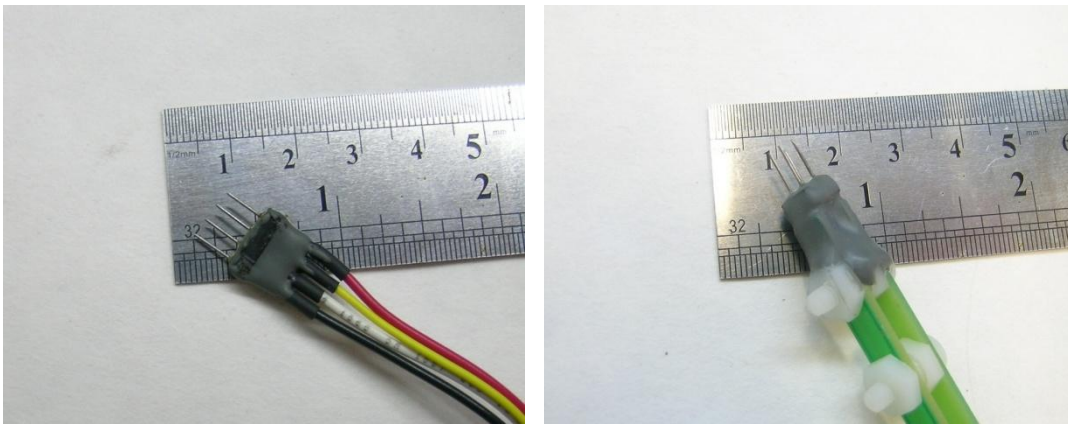

Figure 1: The four electrode devices custom-made for the experiment. (a) The needles are set in a straight line. (b) The needles are set in a square.

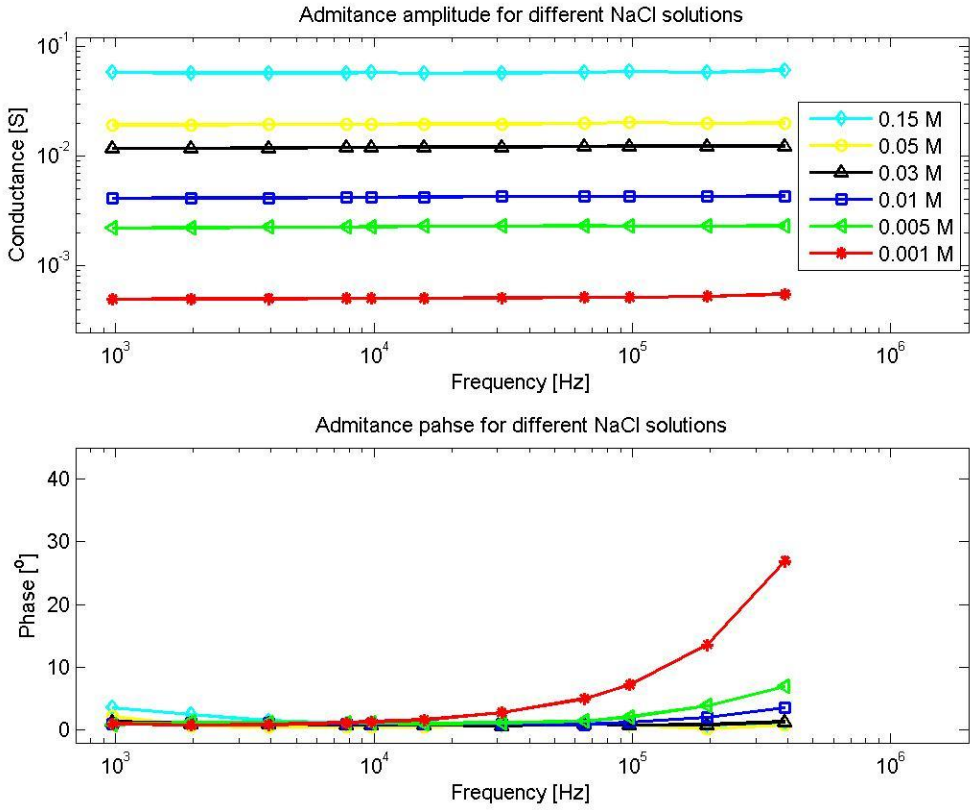


412

413 Figure 2: Admittance of different NaCl solutions measured using electrode (a) for cell
414 constant calculation.

415
416

| NaCl [M] | G [S] average | G [S] SD | G [S] %SD | $\sigma[S\,m^{-1}]$ average | $\sigma[S\,m^{-1}]$ Peyman *et al* | $\sigma[S\,m^{-1}]$ difference (%) |
|---|---|---|---|---|---|---|
| 0.001 | 5.02e-4 / 1.03e-3 | 1.03e-5 / 3.01e-5 | 2.05 / 2.93 | 0.011 / 0.012 | 0.009 / 0.009 | -25.82 / -31.29 |
| 0.005 | 2.26e-3 / 4.26e-3 | 6.87e-5 / 1.53e-4 | 3.04 / 3.59 | 0.051 / 0.049 | 0.047 / 0.047 | -8.42 / -4.36 |
| 0.01 | 4.21e-3 / 8.25e-3 | 9.85e-5 / 3.09e-4 | 2.34 / 3.75 | 0.095 / 0.095 | 0.094 / 0.094 | -0.90 / -1.01 |
| 0.03 | 1.20e-2 / 2.30e-2 | 3.07e-4 / 9.04e-4 | 2.55 / 3.92 | 0.271 / 0.265 | 0.281 / 0.281 | 3.51 / 5.63 |
| 0.05 | 1.96e-2 / 3.90e-2 | 4.84e-4 / 1.81e-3 | 2.48 / 4.64 | 0.441 / 0.449 | 0.466 / 0.466 | 5.38 / 3.70 |
| 0.15 | 5.77e-2 / 1.18e-1 | 2.42e-3 / 1.50e-2 | 4.20 / 12.72 | 1.300 / 1.355 | 1.375 / 1.375 | 5.48 / 1.42 |

Table 1: Evaluation of amplitude accuracy. G [S] is the average conductance from 1 KHz to 400 KHz for different NaCl concentrations. The conductivity is calculated using the average conductance and the cell constant. The values are given for both electrode configurations (needles in straight line / needles in square).

| NaCl [M] | Phase[$^o$] | Phase[$^o$] SD |
|---|---|---|
| 0.001 | 5.66 / 6.96 | 7.78 / 7.89 |
| 0.005 | 2.00 / 2.79 | 1.80 / 1.25 |
| 0.01 | 1.35 / 2.29 | 0.78 / 0.65 |
| 0.03 | 0.95 / 1.79 | 0.28 / 1.26 |
| 0.05 | 0.81 / 1.69 | 0.55 / 2.24 |
| 0.15 | 2.07 / 6.14 | 1.43 / 6.59 |

Table 2: Evaluation of phase accuracy. The phase average and standard deviation from 1 KHz to 400 KHz for different NaCl concentrations. At this frequency range the phase should be approximately zero, i.e., the measured phase is due to equipment errors and electrode artifacts and should be minimized. The values are given for both electrode configurations (needles in straight line / needles in square).

| Frequency [Hz] | $\sigma[S\ m^{-1}]$ difference (%) | Phase[$^o$] |
|---|---|---|
| 976.5625 | 3.30 / 4.06 | 1.84 / 6.66 |
| 1953.125 | 2.85 / 1.58 | 1.36 / 0.68 |
| 3906.25 | 2.38 / 2.08 | 1.07 / 0.44 |
| 7812.5 | 1.70 / 2.07 | 0.89 / 0.73 |
| 9765.625 | 1.58 / 2.99 | 0.95 / 1.06 |
| 15625 | 1.30 / 1.61 | 0.96 / 1.20 |
| 31250 | 0.45 / 1.81 | 0.90 / 1.89 |
| 65104 | 0.05 / 0.79 | 1.06 / 1.97 |
| 97656.25 | -0.90 / 0.40 | 1.16 / 1.94 |
| 195312.5 | -0.23 / -1.37 | 1.53 / 0.35 |
| 390625 | -1.39 / -4.17 | 2.69 / 2.47 |

Table 3: For NaCl concentrations 0.005-0.15 M, for each frequency the average percentage of conductivity difference between the data obtained here and the literature and the average phase (which should be zero).

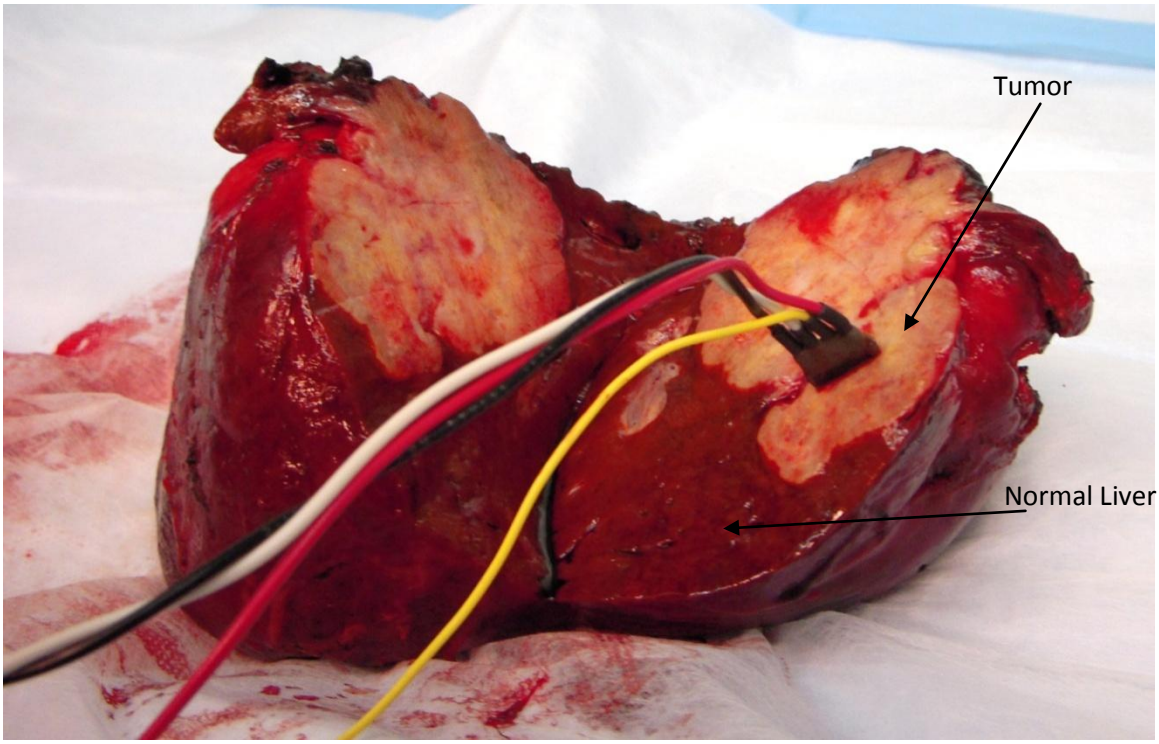


Figure 3 Example of measurement configuration.

| Frequency [Hz] | Normal Conductivity [S/m] | Tumor Conductivity [S/m] | Cirrhotic Conductivity [S/m] | Normal Relative Permittivity | Tumor Relative Permittivity | Cirrhotic Relative Permittivity |
|---|---|---|---|---|---|---|
| 976.6 | 0.030 ±0.01 | 0.166 ±0.08 | 0.105 ±0.02 | 8.2e4 ±2e4 | 9.9e4 ±6e4 | 1e5 ±1e4 |
| 1953.1 | 0.032 ±0.01 | 0.169 ±0.08 | 0.107 ±0.02 | 6.6e4 ±2e4 | 8 e4 ±4e4 | 7.4e4 ±6e3 |
| 3906.3 | 0.035 ±0.01 | 0.173 ±0.08 | 0.110 ±0.02 | 5.2e4 ±1e4 | 5.8e4 ±2e4 | 5.9e4 ±3e3 |
| 7812.5 | 0.040 ±0.01 | 0.179 ±0.08 | 0.116 ±0.02 | 3.8e4 ±9e3 | 3.9e4 ±1e4 | 4.5e4 ±2e3 |
| 9765.6 | 0.042 ±0.01 | 0.181 ±0.08 | 0.119 ±0.02 | 3.5e4 ±8e3 | 3.4e4 ±1e4 | 4e4 ±2e3 |
| 15625.0 | 0.047 ±0.01 | 0.185 ±0.08 | 0.125 ±0.02 | 2.8e4±7e3 | 2.5e4 ±7e3 | 3.2e4 ±1e3 |
| 31250.0 | 0.058 ±0.02 | 0.195 ±0.07 | 0.138 ±0.02 | 2e4 ±5e3 | 1.6e4 ±5e3 | 2.2e4 ±1e3 |
| 65104.0 | 0.076 ±0.02 | 0.209 ±0.07 | 0.155 ±0.02 | 1.3e4 ±3e3 | 1e3 ±3e3 | 1.3e4 ±7e2 |
| 97656.3 | 0.091 ±0.02 | 0.222 ±0.07 | 0.176 ±0.02 | 1.1e4 ±2e3 | 8.6e3 ±2e3 | 1.1 e4 ±5e2 |
| 195312.5 | 0.124 ±0.03 | 0.246 ±0.07 | 0.208 ±0.01 | 6.5e3 ±1e3 | 5.1e3 ±1e3 | 6.2e3 ±3e2 |
| 390625.0 | 0.164 ±0.03 | 0.272 ±0.07 | 0.244 ±0.01 | 3.4e3±5e2. | 3e3 ±6e2 | 3.2e3±2e2 |

444 Table 4 Average conductivity and permittivity of normal, cancerous and cirrhotic tissues.

445

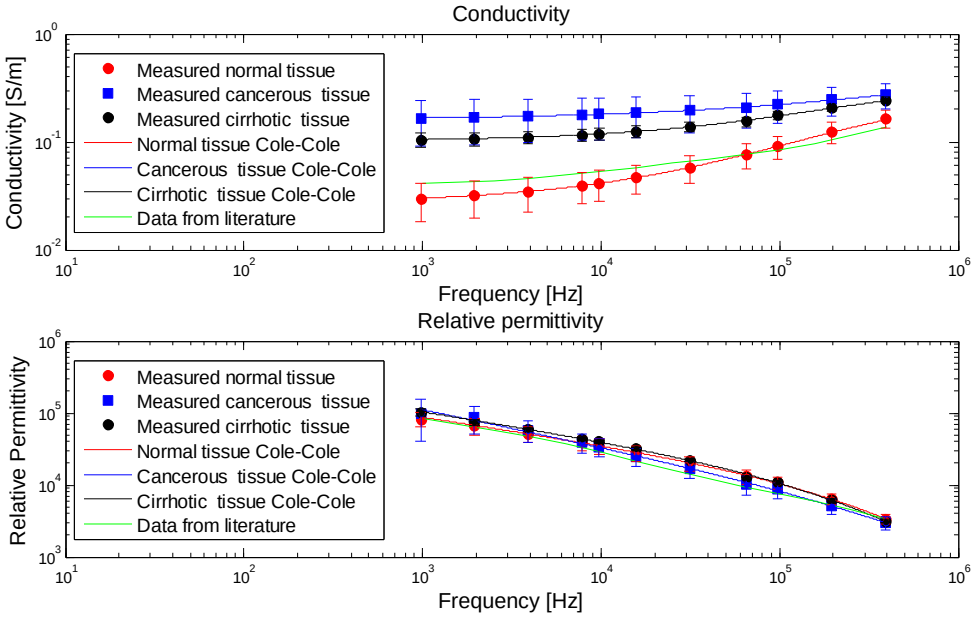


Figure 4: Average conductivity and permittivity of normal, cancerous and cirrhotic tissues. As a reference, data from the literature are presented (Andreuccetti *et al.*, 1997; Gabriel *et al.*, 1996b). The continuous lines are the Cole-Cole model fits for these data with the following parameters:

Normal tissue: $\rho_0$ = 37.26 [Ohm-m] $\rho_\infty$ = 3.31 [Ohm-m] $\alpha$ = 0.634 $f_c$ = 9358 [Hz]

Cancerous tissue: $\rho_0$ = 6.23 [Ohm-m] $\rho_\infty$ = 1.94 [Ohm-m] $\alpha$ = 0.503 $f_c$ = 144731 [Hz]

Cirrhotic tissue: $\rho_0$ = 9.9 [Ohm-m] $\rho_\infty$ = 2.76 [Ohm-m] $\alpha$ = 0.62 $f_c$ =41752 [Hz]

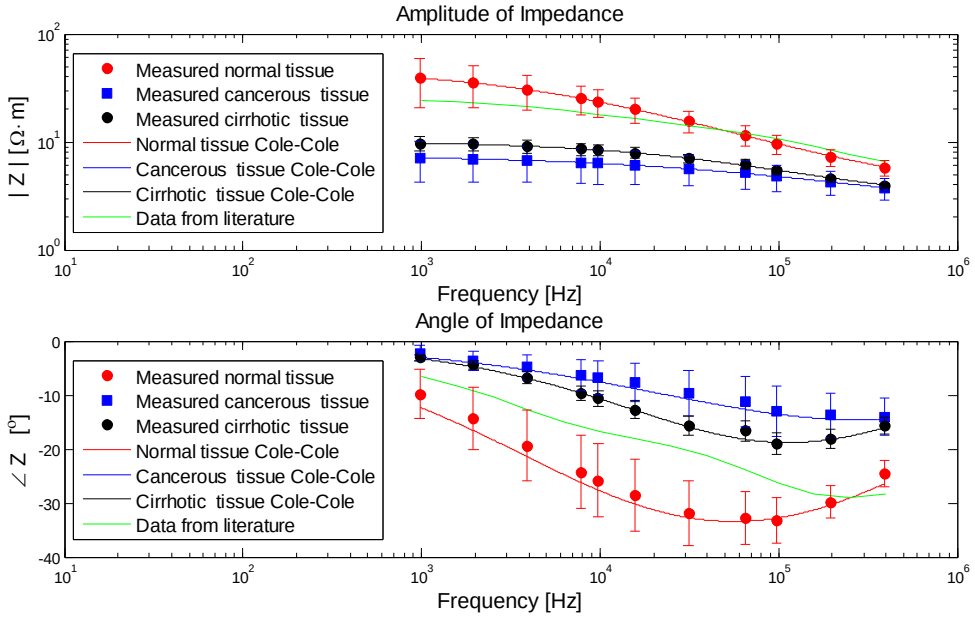


Figure 5: Average impedance amplitude and angle of normal, cancerous and cirrhotic tissues. As a reference, data from the literature are presented (Andreuccetti *et al.*, 1997; Gabriel *et al.*, 1996b). The continuous lines are the Cole-Cole model fits for these data with the following parameters:

Normal tissue: $\rho_0$ = 47.96 [Ohm-m] $\rho_\infty$ = 3.06 [Ohm-m] $\alpha$ = 0.594 $f_c$ = 5567 [Hz]

Cancerous tissue: $\rho_0$ = 7.54 [Ohm-m] $\rho_\infty$ = 2.04 [Ohm-m] $\alpha$ = 0.492 $f_c$ =82294 [Hz]

Cirrhotic tissue: $\rho_0$ = 10.14 [Ohm-m] $\rho_\infty$ = 2.76 [Ohm-m] $\alpha$ = 0.617 $f_c$ =39682 [Hz]

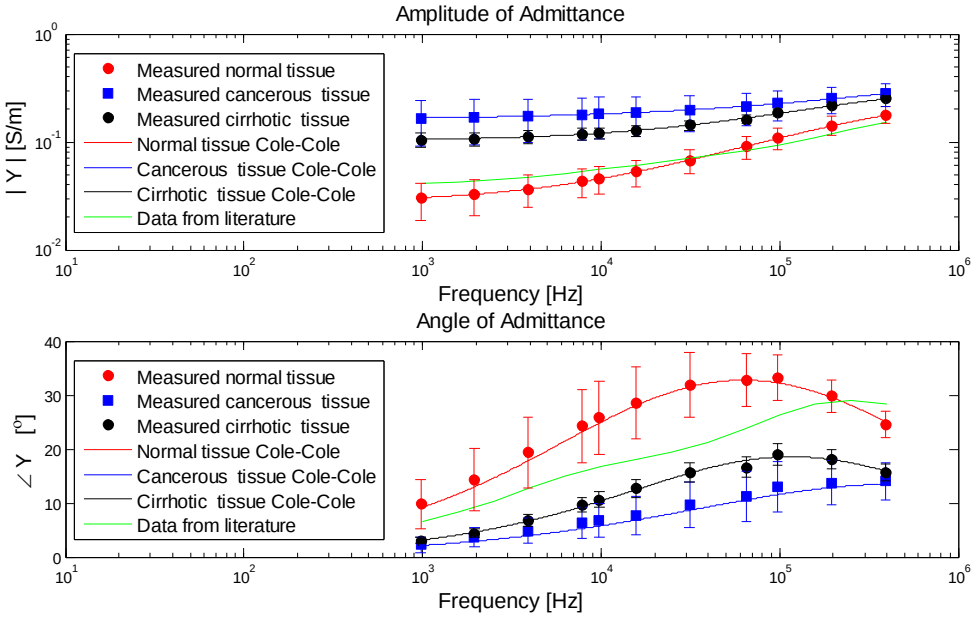


Figure 6: Average admittance amplitude and angle of normal, cancerous and cirrhotic tissues. As a reference, data from the literature are presented (Andreuccetti *et al.*, 1997; Gabriel *et al.*, 1996b). The continuous lines are the Cole-Cole model fits for these data with the same parameters as in Figure 4.

| Parameters | units | Normal | Tumor | Cirrhotic |
|---|---|---|---|---|
| $\rho_0$ | [Ohm-m] | 47.58±28.94 | 7.56 ±3.44 | 10.14 ±1.66 |
| $\rho_\infty$ | [Ohm-m] | 3.29 ±0.65 | 2.15±0.72 | 2.76 ±0.14 |
| $\alpha$ | - | 0.63±0.04 | 0.51±0.14 | 0.62 ±0.02 |
| $f_c$ | [kHz] | 10.5±7 | 155.7±132 | 41.5±8 |

Table 5: Average of the Cole-Cole parameters.

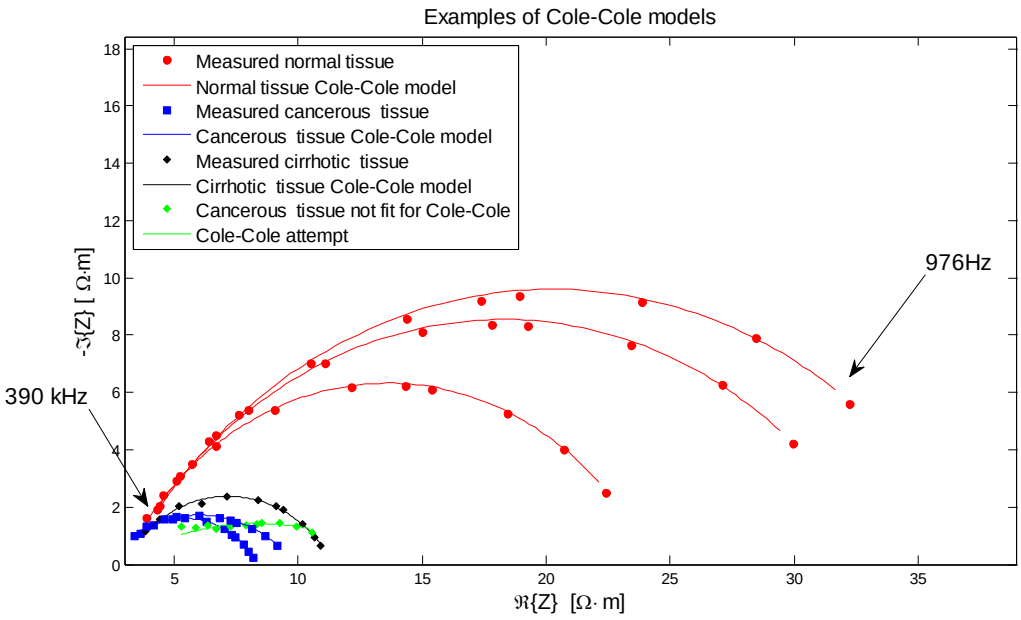


Figure 7: Examples of Cole-Cole models of different tissues.